Coupled Phenomena in Environmental Geotechnics – Manassero et al (Eds)
© 2013 Taylor & Francis Group, London, ISBN 978 1 138 00060 5

Thermal, hydraulic and mechanical performances of enhanced grouting materials for borehole heat exchanger

S. Erol & B. François
Université Libre de Bruxelles, Building, Architecture and Town Planning Dept (BATir), Brussels, Belgium

ABSTRACT: Experimental, numerical and analytical studies are carried out to enhance the thermal performance of vertical ground source heat pump (GSHP) systems by improving the grouting material with the addition of graphite powder. Several mechanical and thermo-physical tests are performed for two different widely used commercial grouting materials (i.e. bentonite-based and silica sand-based) and homemade admixtures enhanced with natural flake graphite, synthetic graphite and expanded graphite. Experimentally to assess the specific heat exchange rates, the prepared borehole heat exchanger (BHE) probes are operated using two heat pumps in a $1 \times 1 \times 1\,m^3$ sandbox under dry (solid – air) condition. The home-made admixture prepared with 5% natural flake graphite can be considered as an appropriate grout material for BHEs regarding to its rheological and thermo-physical properties as well as its cost. During the operations, the monitored temperature measurements in the sandbox are in agreement with numerical simulation and analytical approach prediction. The sandbox study shows that if the thermo-physical properties of ground is considerably low, the thermal conductivity of grout has no significant impact on the performance of BHE, the main resisting component in the thermal transfert being the ground itself.

1 INTRODUCTION

Geothermal energy is the form of energy that is extracted from the stored heat ground, and within a range of 0 to 400 m of depth the stored heat is categorized as shallow geothermal energy. In order to use this energy, there are varieties of different earth-coupled heat extraction systems. The closed-loop geothermal system is one of the mostly used technologies and its configuration comprises a heat exchanger installed inside a borehole and a pump that circulates a solution of water or anti-freeze mixture through the buried pipes. Thus, the heat is transferred from the ground to the heat carrier fluid. The objective is to maximize the heat transfer, in order to optimize the performance of the system.

The GSHP systems for domestic heating and cooling are basically installed in the ground with high density polyethylene (HDPE) pipes and filled the surrounding empty space mostly with grout inside the borehole (e.g. in Sweden groundwater can be used as filling material). In addition to the thermo-physical and hydro-geological conditions of the ground, the characteristics of backfill materials, particularly thermal conductivity, may play an important role for the specific heat exchange rate (Jun et al. 2009; Lee et al. 2011).

In order to improve the specific heat exchange rate of BHEs, thermal conductivity of the grout material can be enhanced. Particularly, graphite-based admixtures (Lee et al. 2010; Lee et al. 2011; Delaleux et al. 2012) have been investigated to enhance the thermal conductivity of grouting material. Lee et al. 2010 experienced on the suitability of different type of grouting materials for BHEs. They indicated that with increasing the content of silica-sand and graphite in an admixture, the thermal conductivity rises, however, the viscosity of the admixture also increases. As a result, by adding 30% graphite to bentonite-based admixture led to a thermal conductivity of $\sim 3.5\,W\,m^{-1}\,K^{-1}$. In addition, Lee et al. 2011 experienced several in-situ thermal response tests (TRT) to study the performance of the vertical GSHP systems with considering various grouting materials. They developed an admixture containing cement, silica-sand and graphite providing a thermal conductivity of $\sim 2.6\,W\,m^{-1}\,K^{-1}$. Recently, Delaleux et al. 2012 claimed that by adding less than 15% graphite powder in an admixture, the enhancement of grout thermal conductivity can be led to a significant increase of the specific heat exchange rate regarding to present commercial backfilling materials. Nevertheless, in most of the previous works, other necessary parameters such as permeability, compression strength and workability, were not determined to proof the applicability of those admixtures as a grouting material.

The main objective of the present research is to focus, not only on the thermal improvement, but also on the other rheological properties of the grout in order to guarantee a proper behavior of the BHE. Several laboratory tests have been performed to determine the suitability of grouting materials for BHE

and a small-scale sandbox TRT have been operated in the laboratory for two different commercial products (bentonite-based and silica sand-based) and one of the home-made admixtures containing natural flake graphite. In addition, numerical and analytical studies are carried out to compare the sandbox test results, and also to evaluate the specific heat exchange rate and the thermal resistances of BHE.

2 ADMIXTURE

2.1 *Commercial grouting materials*

In order to investigate the range of specific heat exchange rate depending on the typical characteristics of grouting materials, first analyses are carried out by considering two different commercial products that have been used as backfilling material for BHEs. One of the considered products is bentonite-based ($\sim 0.9\,W\,m^{-1}\,K^{-1}$) and other is silica sand-based ($\sim 2.3\,W\,m^{-1}\,K^{-1}$). Those two products have been chosen for their relatively high difference in thermal conductivity, in order to have a large range of selection. The objective is to justify how the grouting materials drive the heat exchange rate.

2.2 *Homemade admixtures*

The considered graphite types for the pre-analyses (i.e. mechanical and thermo-physical tests) are listed by increasing cost: (1) natural flake graphite (TIMREX M100/45–150 μm), (2) the primary synthetic graphite with two different grain size distribution (TIMREX KS150/150 μm, TIMREX KS150-600/150 – 600 μm), and (3) expanded graphite powder (TIMREX C-THERM011/2.5% ashes) (TIMCAL 2012). The components are mixed with various ranges (5–12% graphite, 24–40% silica sand ($D50 = 260\,\mu m$), 24–45% water, 20–28% cement and 0–7% Ca^{2+} bentonite), in order to determine the fraction contents of admixtures. According to the preliminary (visual) observations, and also regarding to the guidelines VDI 4640 (Blatt – 2 & 3) and Allan & Philippacopoulos (1998; 1999), the proportion of graphite shall be less than 10% and silica sand should not exceed 50%, because graphite absorbs large amount of water and with the addition of silica sand the pumpability of admixture becomes unfeasible due to its high viscosity (VDI 2001b). Therefore, the amount of graphite powder is kept 5% in all prepared home-made admixtures.

3 THERMO-PHYSICAL, HYDROLOGICAL AND MECHANICAL CHARACTERIZATION OF GROUT MATERIALS

The principal tasks about the grouting materials are to provide a good thermal conduction between the pipes and surrounding ground and to ensure a watertight, durable and frost-proof material (Hermann 2008; Reuß et al. 2011). In order to propose an appropriate grouting material in accordance with guidelines, the characteristics of grouting materials must be determined in terms of hydraulic conductivity, uniaxial compression strength, thermal conductivity and workability.

The allowable permeability of backfilling material shall be $\leq 1 \times 10^{-9}\,m\,s^{-1}$ (GSHPA 2011). The permeability has been measured in falling head permeameter.

The considered grouting materials are placed inside the cells, when they are fresh. Then the samples are left for curing for 2 weeks under water. Then the falling hydraulic head in the pipe is measured through 30 days to calculate the permeability. Thereby, the permeability can be evaluated as a function of curing time.

The uniaxial compression test is the estimation of the compression strength of a grouting material with unrestricted horizontal deformation.

Before compression strength tests, the prepared fresh samples are placed in a humidity room (~80% humidity) under constant temperature at 20°C, and curing time is set to 10 days and 30 days to observe how the strength of the materials changes in time.

Thermal conductivity of grouting material is determined with the thermal needle probe device (1.5 mm diameter and 150 mm length).

While the admixture material is fresh, a thin rigid stick that has the same diameter then the needle probe (1.5 mm) is placed in the middle of sample (cylinder shaped sample $d = 100\,mm$, $h = 200\,mm$). Thereby, the needle probe can be replaced into the sample when it is dried. During the thermal conductivity measurement, the surrounded gap between the sample and the needle is filled with a highly-conductive thermal paste ($\sim 5.6\,W\,m^{-1}\,K^{-1}$) to avoid artifacts due to air included in the gap.

For determining the pumpability and the plastic viscosity of admixtures characterizing its workability, the flow cone method, so called Marsh cone is performed.

The specified volume of fresh grout, 1725 mL, flows through the nozzle of the cone, and the time of efflux of suspension is measured in seconds. In Roussel & Le Roy (2005), an empirical method is described to classify the flowability of different suspensions. The represented criterion is related to several rheological parameters (i.e. plastic viscosity and yield stress) which can be calculated depending on the efflux time, density of grout and cone geometry (e.g. height of the cone, radius of the nozzle).

4 SMALL-SCALE BHE CHARACTERIZATION

4.1 *Sandbox description*

The small-scale TRT experiment is carried out under dry sand (solid – air) condition. The size of the considered sandbox for the experiments is $1 \times 1 \times 1\,m^3$. The initial ground temperature is 20°C. The BHEs with a diameter of 0.135 m are operated with two heat pumps

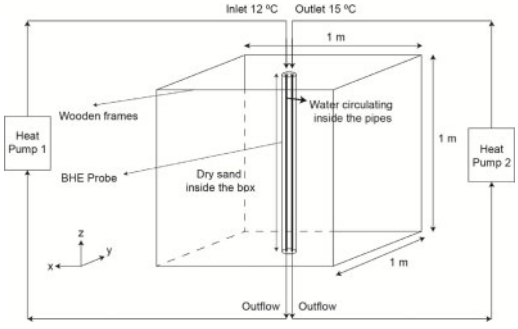

Figure 1. The illustration shows the procedure of small scale sandbox TRT operated with two separated heat pumps.

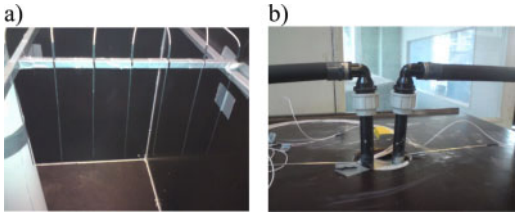

Figure 2. The considered locations of the thermistors for temperature measurements: a) 7 pieces thermistor along the y-axis of a BHE with an interval distance of 7.2 cm b) Thermistors inside the pipes.

that circulate water with temperature fixed at 12°C (inlet) and at 15°C (outlet), respectively (Fig. 1). In a real operation, the pump circulates the fluid through the geothermal probe (~100–200 m) to have a thermal gradient between inlet and outlet by the heat exchange with the ground. In the present test, the 1 m probe length is not enough to produce a significant temperature difference between inlet and outlet (~3°C). Therefore, the fluid temperatures in the two pipes are controlled separately.

The outer diameter of the pipes is 0.032 m, and the flow rate is set to 3.66×10^{-4} m^3/s (turbulent flow with the Reynold number of 1.1×10^4). As the boundary conditions, we isolated properly the sandbox and the pipes from the probe to the heat pumps. The operation time is set to the minimum suggested duration of a TRT, 50 hours (Austin et al. 2000; Gehlin 2002), because the ambient temperature strongly influences the temperature distribution inside the sandbox in case of the longer operations and also after 50 hours, the radius of influence of the BHE reaches the wall of the box.

Since the temperature distribution is symmetric in the sandbox due to conduction dominated heat transfer system, the temperatures are measured along the y axis of BHE with the pt-100 precision thermistors. Additionally, two thermistors are placed inside the pipes where the fluid flow into the BHE, to correct the temperature difference between the heat pump and the probe (e.g. heat pump set 11.7°C the thermistor read 12°C).

The widely used method to estimate specific heat exchange rate Q of the BHE is based on the temperature difference between inlet and outlet (in our case, the sum of the temperature difference of the inflow and the outflow of each pipe) given as follows:

$$Q = \frac{\rho_f c_f q_f \left(\Delta T_1 + \Delta T_2\right)}{L} \quad (1)$$

in which $\rho_f c_f$ is volumetric heat capacity of heat carrier fluid, q_f is the flow rate, ΔT_1 and ΔT_2 denote the temperature variation of the fluid in the pipes 1 and 2 along the 1 m probe length, L.

However, since the temperature difference of the fluid between inflow and outflow of each pipe is considerably small (<0.1°C) for a BHE with a 1 m length, it is not possible to obtain precision measurement data due to both the sensor accuracy and the resolution of the acquisition device, ±0.03°C and ±0.1°C, respectively. Therefore, it appears best to estimate the specific heat exchange rate with the evaluation of decreasing sand temperature.

Line source or cylindrical source models can be adopted to evaluate the thermal characteristics of the ground by using in-situ TRT data. Most of the time, those approaches are used to deduce the thermal properties of the ground, controlling the heat input. However, reversely, it is also possible, knowing the ground properties, to deduce the specific heat exchange rate through back-analysis. This is what will be done in chapter 4.2.3 based on the temperature profile in the sand.

4.2 *Analytical solution*

The objective to use an analytical solution is to gain time for long-term prediction of an engineering application, and this implemented analytical approach can provide us to investigate the near field behavior of a BHE such an operation of 30 years.

Infinite and finite analytical solutions for BHEs consider mostly conduction dominated systems (Ingersoll et al. 1954; Carslaw & Jaeger 1959). However, those assumptions consider a constant heat load and do not take into account the borehole resistances to calculate the temperature change in the surrounding ground. Since we fix the mean fluid temperature to a certain value, the heat input changes as a function of time. Therefore, we should impose several backward computations to estimate the temperature difference in the vicinity of BHE. First, the borehole resistances and the heat input rate are analytically calculated as a function of time. Then the computed heat load, $q(t)$, is obtained as a function of borehole resistance and mean fluid temperature.

4.2.1 *Borehole resistance*

The borehole resistances can be analytically estimated regarding to its geometry factor and its typical characteristics. It accounts for the convection and conduction

pipe resistances and effective borehole wall resistance (Lamarche et al. 2010):

$$R_b = \frac{\left(T_f(t) - T_b(r_b,t)\right)}{Q} = \underbrace{R_{conv}^{'} + R_{cond}^{'}}_{R_{pipe}} + R_b^{'} \tag{2}$$

The total borehole thermal resistance R_b corresponds to the temperature difference between the mean fluid temperature T_f and the borehole wall temperature T_b divided by the specific heat exchange rate Q. This total borehole thermal resistance includes pipe resistance R_{pipe} (decomposed into convection and conduction resistance R'_{conv} and R'_{cond}, respectively) and grout thermal resistance R'_b. The two pipe resistances, the convection resistance:

$$R_{conv}^{'} = \frac{1}{4\pi r_i h} \tag{3}$$

$$h = \frac{\mathrm{Nu}\lambda_f}{d_i} \tag{4}$$

$$R_{cond}^{'} = \frac{\ln\left(r_o / r_i\right)}{4\pi\lambda_{pipe}} \tag{5}$$

in which r_i and r_o are the inner and outer radius of pipe, respectively, and h is the heat transfer coefficient estimated with Nusselt number (Nu), inner diameter of the pipe d_i and thermal conductivity of the fluid λ_f.

The third contribution of Eq. 2 is a 2D grout thermal resistance. There are different equations to calculate the grout thermal resistance excluding pipe resistance (Hellström 1991; Paul 1996; Sharqawy et al. 2009). In particular, Bennet et al. (1987) used the multipole method. Lamarche et al. 2010 shows that among other approaches under steady-state and transient conditions, the multipole solution provided the best estimation with regard to the numerical results. For single U-shaped pipe, the first-order solution is given as follows Bennet et al. (1987):

$$R_b^{'} = \frac{1}{4\pi\lambda_{grout}}\left[\ln\left(\frac{\alpha_1\alpha_2^{1+4\sigma}}{2\left(\alpha_2^4-1\right)^{\sigma}}\right) - \frac{\alpha_3^2\left(1-\dfrac{4\sigma}{\left(\alpha_2^4-1\right)}\right)^2}{1+\alpha_3^2\left(1+\dfrac{16\sigma}{\left(\left(\alpha_2^4-1\right)/\alpha_2^2\right)^2}\right)}\right] \tag{6}$$

in which $\alpha_1 = r_b / r_p$, $\alpha_2 = r_b / x_c$, $\alpha_3 = r_p / 2x_c$ and r_b is the radius of borehole 0.0675m, r_p is the external radius of pipe 0.016 m and x_c is the shank space 0.0415 m. σ is given as follows:

$$\sigma = \frac{\lambda_{grout} - \lambda_{soil}}{\lambda_{grout} + \lambda_{soil}} \tag{7}$$

4.2.2 *Heat input rate*

In the following step, the calculated borehole resistance is taken into account in Eq. 8 to calculate the heat input rate as a function of time, in order to keep the mean fluid temperature as a constant in time. Essentially, the equation 8 is used to evaluate the mean fluid temperature as a function of time by taking line source method devivated by Carslaw & Jaeger 1959 and adding the effective borehole resistance (Gehlin 2002). In our case, we solve backward this equation to calculate the heat input rate as a function of time:

$$q(t) = \frac{\left(T_0 - T_f\right)}{\dfrac{1}{4\pi\lambda_{soil}}\left(\ln\left(\dfrac{4at}{r_b^2}\right) - \gamma\right) + R_b} \tag{8}$$

where a is the thermal diffusivity, T_0 is the undisturbed soil temperature, and γ is the Euler constant, that is typically ~0.57721.

4.2.3 *Temperature distribution in the ground*

In the last step, the calculated heat input rate as a function of time can be taken into account for one of the line source model. We used the moving finite line source method (MFLS) for a vertical BHE derivated by Molina et al. 2011 that considers both the axial effect and groundwater flow. The MFLS agrees well with numerical results under steady-state and transient (groundwater flow) underground conditions for short (>2 hour) and long-term (e.g. 40 years) simulations. The MFLS method is given as follows:

$$\Delta T(x,y,z,t) = \frac{q(t)}{2\pi\lambda_{soil}}\exp\left[\frac{v_T x}{2a}\right] \times\left[\int_0^H f(x,y,z,t)\,dz' - \int_{-H}^{0} f(x,y,z,t)\,dz'\right] \tag{9}$$

in which v_T is the effective heat transport velocity depending on the seepage velocity (in our study it is zero), $f(x,y,z,t)$ is derivated as:

$$f(x,y,z,t) = \frac{1}{4R}\left[\exp\left(-\frac{v_t R}{2a}\right)erfc\left(\frac{R - v_t t}{2\sqrt{at}}\right)\right] + \left[\exp\left(\frac{v_t R}{2a}\right)erfc\left(\frac{R + v_t t}{2\sqrt{at}}\right)\right] \tag{10}$$

R is the distance to the source placed on z-axis in 3D Euclidean space and expressed as:

$$R = \sqrt{x^2 + y^2 + \left(z - z'\right)^2} \tag{11}$$

Knowing the experimental temperature distribution, Eq. 9 can be solved backward to deduce $q(t)$, which is specific heat exchange rate Q (including thermal transfer and borehole resistance). One of the temperature measurement in the sandbox at where the temperature distribution is symmetric can be taken into account for $\Delta T(t)$ to calculate the specific heat

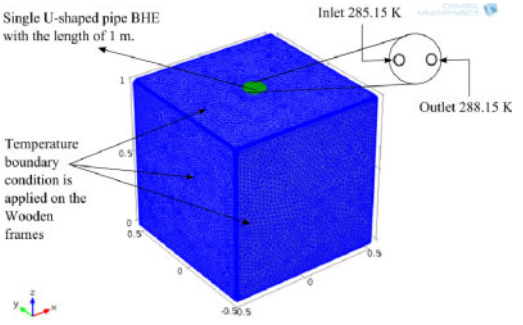

Figure 3. 3D model domain with a 1 m length of BHE.

Table 1. Characteristics of the pipe, water, air and silica sand.

Parameters	Thermal conductivity [W m^{-1} K^{-1}]	Specific heat capacity [J kg^{-1} K^{-1}]	Density [kg m^{-3}]
Pipe*	0.42	2170	960
Water**	0.59	4185	1000
Air**	0.024	1000	1.25
Silica sand (air/solid)§	$\sim$ 0.35†	820**	1500**

*(Hakagerodur-geothermal 2012), **(Engineering toolbox 2012), §Bulk thermal properties of sand with the porosity of 0.43 [–] (Sibelco 2012), †measured value.

exchange rate (T at x = 0 m, y = 0.14 m, z = 0.5 m), and the borehole resistance is estimated according to the left-hand side of the equation 2 (T_b at x = 0 m, y = 0.0675 m, z = 0.5 m).

4.3 *Numerical model*

The objective of numerical model is to understand the impact of the components on the heat transfer system (i.e. grout, pipe, soil). The study is represented by a 3D homogeneous model domain (Fig. 3) with the finite element software program COMSOL Multiphysics. The model domain is set according to the sandbox size (interior dimensions 1 m × 1 m × 1 m). Since the ambient temperature influences the measurement during the operations, the wooden frames with the thickness of 1.3 cm are also fixed to the model domain. The mesh is generated using uniform triangle elements. The BHE is located at the central position of the model domain.

As the boundary conditions, temperature boundary condition is applied on the modeled wooden walls from each side according to the recorded outer wall temperature (between the isolation material and wood frame). Other parameters (i.e. inlet, outlet and simulation time) are set according to the sandbox experiment (Chapter 4.1). For the simulations, groundwater flow is not considered. The provided parameters of silica sand shown in Table 1 is set to the model as the bulk thermal properties of the porous media (air/solid phase).

5 RESULTS

5.1 *Laboratory test results*

The fundamental comparison of all variant results can be found in Table 2. As the reference measurement, the results of two commercial products are nearly in agreement with the values provided by the producers. However, during the process of sample preparing, because of brittleness of C-2 bentonite-based grout, micro cracks were produced, that could alter the results for compression strength and thermal conductivity.

Compared the results of home-made grouts with the reference values of the commercial grouts, permeability, density and compression strength results are in an allowable range, except the result of admixture prepared with expanded graphite A-5 for which permeability $\leq 1 \times 10^{-9}$ m/s is not fulfilled, and the lowest compression strength and density is observed among other grouts. The reason is the expanded graphite has lower density than the other graphite powders (e.g. expanded graphite bulk density = 150 kg m^{-3}, synthetic graphite 150–600 μm bulk density = 670 kg m^{-3}).

The higher fraction of sand in A-1 (40%) and the larger size graphite grains (> 300 μm) which are sunk into the bottom of A-4 sample caused the sedimentation in those admixtures. Except the admixtures A-1 and A-4, other suspensions are mixed homogeneously.

Compared the Marsh cone test results, the flowability of A-1 and A-4 admixtures are considerably faster than other home-made grouts, because the well-graded grain size distribution decreased both the yield stress and the plastic viscosity of those suspensions. On the other hand, the efflux of silica sand-based grout and C-2 bentonite-based w/b = 0.5 is stopped in the Marsh cone after several drops, even if they are homogeneous mixtures. The flow time of bentonite-based grouts is decreasing with rising w/b ratio due to decreasing viscosity. The calculated plastic viscosity results are proportional to the efflux time of all admixtures and vary depending on the component characteristics of grouts (e.g. grain size distribution of components).

Currently, the thermal conductivity results of only three home-made admixtures and two commercial products are available. Even, the existing results of home-made admixtures demonstrate that 5% addition of graphite has a significant impact on the thermal conductivity of grout (e.g. A-1 without graphite = 1.5 W m^{-1} K^{-1}, A-2 with natural graphite = 2.3 W m^{-1} K^{-1}).

In Figure 4, after a flat first part of the curve (corresponding to the closure of the gap between the loading piston and the sample), uniaxial compression curves give a straight line that demonstrates the elastic behavior of the grouts. Then, under high load, nonlinear curve shows plastic behavior. The compression strength of each material is taken as the peak value of each curve. When C-2 bentonite-based grouts reach its elastic limit, then a sudden failure occur that is the characteristic of brittle response. On the contrary,

Table 2. Measured parameters for two commercial grouting materials and home-made admixtures.

Admixtures	Permeability [m s^{-1}]	Density [kg m^{-3}] $\times 10^3$	Plastic viscosity§ [Pa s]	Marsh cone† [s/1725 mL]	Compression strength [N mm^{-2}]	Thermal conductivity [W m^{-1} K^{-1}]
C-1 silica sand-based	$<1\times10^{-9\dagger}$ /6×10^{-10}*	$\sim$1.8‡/$\sim$ 1.8**	–	No flow	10‡/9.3**/3.8‡	2.35‡/2.3**
C-2 bentonite-based w/b = 0.5	$<1\times10^{-10\dagger}$/4.3×10^{-12}*	$\sim$1.7**	–	No flow	–	–
C-2 bentonite-based w/b = 0.6	$<1\times10^{-10\dagger}$/9×10^{-12}*	1.66‡/$\sim$1.66**	$\sim$0.20	25 ± 1	8.5‡/5.2**/3.1‡	0.95‡/0.7**
C-2 bentonite-based w/b = 0.7	$<1\times10^{-10\dagger}$/8.1×10^{-11}*	1.6‡/$\sim$1.6**	$\sim$0.13	17 ± 1	–	–
C-2 bentonite-based w/b = 0.8	$<1\times10^{-10\dagger}$/2.8×10^{-10}*	1.55‡/$\sim$1.54**	$\sim$0.11	14 ± 1	–	–
A-1 without graphite	2.8×10^{-12}*	$\sim$1.75**	$\sim$0.23	27 ± 1	8.2**	1.5**
A-2 with natural graphite	4.4×10^{-12}*	$\sim$1.7**	$\sim$0.6	72 ± 1	8**	2.3**
A-3 with sythetic graphite 150 μm	2.2×10^{-12}*	$\sim$1.75**	$\sim$0.41	48 ± 1	10**	2.5**
A-4 with sythetic graphite 150–600 μm	3.3×10^{-12}*	$\sim$1.75**	$\sim$0.19	22 ± 1	9.8**	–
A-5 with expanded graphite	$>1\times10^{-3}$*	$\sim$1.2**	$\sim$0.36	61 ± 1	1.7**	–

*Measured values after the curing period of 45 days (cured under water), **and ‡Values are the average of two samples and measured values after the curing period of 30 days and 10 days, respectively (cured under 80% humidity at constant temperature 20°C), ‡values provided by producers, §backward calculations based on efflux time, density and the properties of Marsh cone geomerty (Roussel & Le Roy 2005), †radius of nozzle 5 mm, cone angle $\tan(\alpha) = 0.253$.

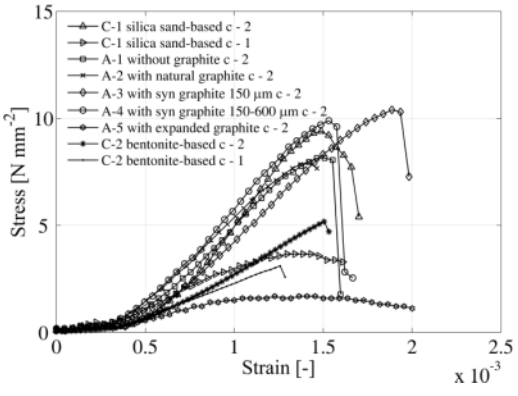

Figure 4. Comparison of the compression strength results between all grouts. w/b ratio of bentonite-based grout is 0.6. c – 1 presents the curing period of 10 days and c – 2 denotes 30 days. Soil type is dry sand (air – solid).

C-1 silica sand-based grout exhibits plastic hardening behavior, when the stress exceeds its elastic limit. After the peak point of the loaded stress, C-1 silica sand-based grout fractured. The results of home-made admixtures (A-1 to A-5) provide nearly identical elastic behavior, except the admixture A-5. Obviously, the density and the texture of expanded graphite have a negative impact on the plastic behavior and ultimate strength.

Concerning the curing period of samples (currently only for commercial grouts), the samples performed for the test after 10 days (c – 1) fractured under less pressure than other samples cured for 30 days (c – 2).

5.2 *Sandbox experiment results*

Three different probes are prepared for the operations. Two probes are made with the commercial grouts, C-1 silica sand-based ($\lambda = 2.3$ W m^{-1} K^{-1}) and C-2 bentonite-based ($\lambda = 0.9$ W m^{-1} K^{-1}), to observe the influence of grout thermal conductivity on the heat transfer. In addition, the third probe is made with A-2 admixture containing natural graphite ($\lambda = 2.3$ W m^{-1} K^{-1}) to compare with other two commercial grouts, because based on thermo-hydro-mechanical laboratory analysis this admixture seems to be the most efficient home-made grout regarding to the cost aspect and the laboratory test results.

Figures 5 and 6 demonstrate the temperature distribution in the sandbox over distance and over time, respectively for operated BHE probe prepared with C-1 silica-sand based grouting material. The room temperature during the test was in the range of 19.8°C to 21.6°C. In both figures, the numerical simulation results are nearly identical respect to the experimental measurements, and the root mean square errors (RMSE) between numerical and experimental results are 0.091 and 0.075, respectively. On the other hand, the analytical solution result is slightly apart from the experimental measurement (RMSE = 0.154 and 0.114, respectively). The reason is that we cannot consider the boundary conditions (i.e. the influence of room temperature) on the analytical solution as

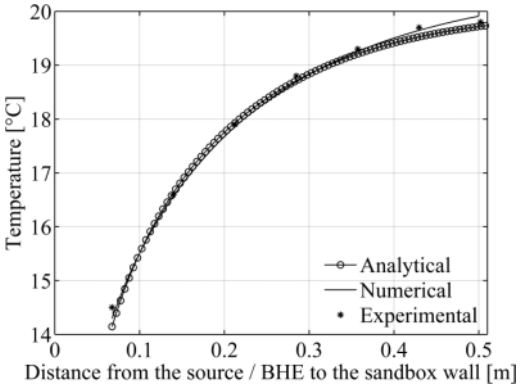

Figure 5. Comparison of experimental measurement with numerical and analytical (Eq. 13) solution results at 50th operation hour (x = 0 m, y = 0.0675 m − 0.5 m, z = 0.5 m) for BHE probe prepared with C-1 silica sand based grouting.

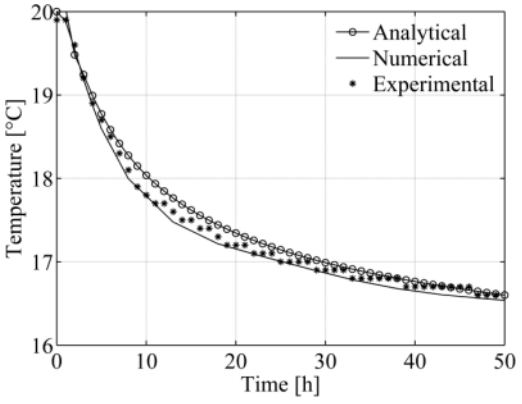

Figure 6. Comparison of experimental measurement with numerical and analytical (Eq. 13) solution results over time (x = 0, y = 0.14 m, z = 0.5 m) for BHE probe prepared with C-1 silica sand based grouting.

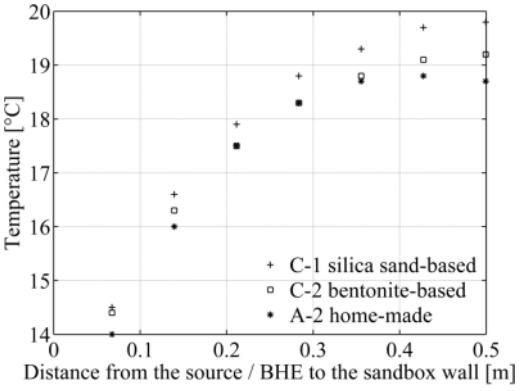

Figure 7. Comparison of experimental results at 50th operation time hour (x = 0.5 m, y = 0.0675 m − 0.5 m, z = 0.5 m).

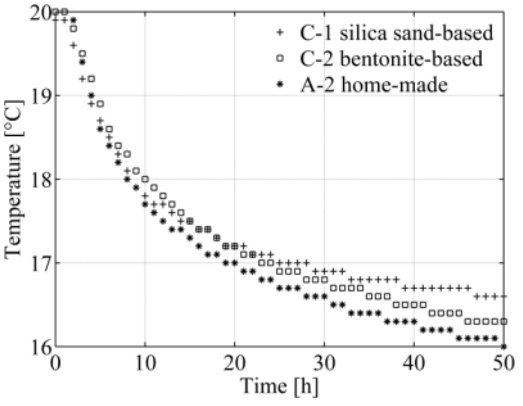

Figure 8. Comparison of experimental results over time (x = 0.5, y = 0.14m, z = 0.5 m).

well as we did on the numerical model according to the temperature measurements on the sandbox wall. Therefore, a small discrepancy between analytical solution and the experimental data is observed.

In Figure 6, the plateau view of the experimental results can be accounted for the acquisition card connected to the thermistors. This problem can be seen also in Figures 8 and Figure 9.

Figures 7 and 8 show the comparison of temperature results obtained with different grout materials. In Figure 7, the influence of room temperature on the sandbox wall can be seen, particularly, on the results of C-2 and A-2. Similarly, we observe a contrariety in Figure 8 between the results. Regarding to the initial temperature, the bentonite-based probe essentially cannot affect the temperature difference in the sandbox more than other two probes due to less thermal conductivity of grout C-2. Actually, the slight difference between three curves is mainly due to the ambient temperature effect. The thermal properties of grouting materials does not have a predominant effect because of the poor thermo-physical properties of the soil (e.g. bulk volumetric heat capacity of soil = 1.3×10^6 J m^{-3} K^{-1}, thermal conductivity = 0.35 W m^{-1} K^{-1}) in which the main resistance for thermal transfer takes place. The heat exchange is dominated by the soil thermal characteristics rather than the thermal conductivity of grout and the three grouting materials provides similar performance in term of heat exchange rate, as demonstrated in Figure 9.

In Figure 9, the specific heat exchange rate and the borehole resistance are calculated from Eq. 9 and Eq. 2, respectively (Chapter 4.2). As explained in the previous paragraph, the results demonstrate also that under dry sand conditions the thermal conductivity of grout has no important role on the specific heat exchange rate due to low thermo-physical properties of soil. Considering the borehole resistances, the mean R_b value of A-2 home-made admixture shown in Figure 9 is lower than C-1 commercial grout. Since the thermal conductivity of grout is one of the major dependence of the borehole resistance, the thermal conductivity of A-2 may be higher than C-1. However, according to the

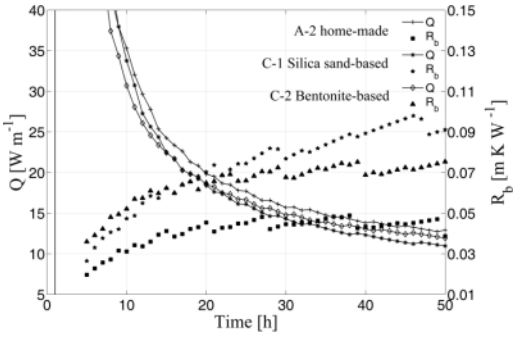

Figure 9. Comparison the performance of C-1 silica sand-based and C-2 bentonite-based and A-2 home-made grouting materials. Soil type is dry (air – solid) sand.

laboratory measurements of grouts, the thermal conductivity of C-1 and A-2 grout materials is identical (Table 2).

6 CONCLUSION

The grouting material used for BHEs must guarantee several hydraulic, mechanical and thermo-physical requirements. The present study provided a wide investigation on the various admixtures with laboratory tests and comprehensive evaluation of the performance of BHE probes based on different type of grout materials by the experimental, numerical and analytical analyses.

Regarding to the laboratory test results, it is conclude that even a small amount of graphite addition (5%) has a great influence on the thermal conductivity of grout. However, it is not feasable to use all kind of graphite powders in an admixture used as a backfill material of BHEs, because different specific characteristics of graphite affect adversely the mechanichal behaviors of grouts (e.g. low permeability and compression strength). In fact, the home-made admixture prepared with 5% natural flake graphite can be considered as an appropriate grouting material for BHEs regarding to the laboratory results and the cost aspect.

Considering the sandbox experiments, if the thermo-physical properties of ground is considerably low (e.g. dry soil), the thermal conductivity of grout has no significant impact on the specific heat exchange rate. This has been demonstrated by both experimental and analytical/numerical simulations.

As the further steps to determine the impact of highly conductive heat transfer system on the performance of BHE, the probes will be operated under water-saturated sand condition ($>2\,W\,m^{-1}\,K^{-1}$).

ACKNOWLEDGEMENT

The financial support from Walloon Region in Belgium is profoundly acknowledged. Furthermore, the authors would like to thank the company Schwenk GmbH Germany, TIMCAL Ltd. Switzerland and Sika group Belgium for raw materials.

REFERENCES

Allan, M.L. & Philippacopoulos, A.J. 1998. *Thermally conductive cementitious grouts for geothermal heat pumps*. FY 98 Progress Report, BNL 66103.

Allan, M.L. & Philippacopoulos, A.J. 1999. *Properties and performance of thermally conductive cement-based grouts for geothermal heat pumps*. FY 99 Final Report.

Austin, W.A., Yavuzturk, C., Spitler, J.D. 2000. Development of an in-situ system for measureing ground thermal properties. *ASHRAE Transactions*. 106(1): 365–379.

Bennet, J., Claesson, J., Hellström, G. 1987. *Multipole Method to Compute the Conductive Heat Transfer to and between Pipes in a Composite Cylinder.* Notes on Heat Transfer 3. Lund: Lund Institute of Technology.

Carslaw, H.S. & Jaeger, J.C. 1959. *Conduction of Heat in Solids, second edition*. New York: Oxford University Press.

COMSOL 2012. COMSOL 4.2a, Multiphysics Modeling, Finite Element Analysis and Engineering Simulations Software, COMSOL, Inc., Burglington, MA.

Delaleux, F., Py, X., Olives R., Dominguez, A. 2012. Enhancement of geothermal borehole heat exchangers performances by improvement of bentonite grouts conductivity. *Applied Thermal Engineering* 33–34: 92–99.

Engineering Tool Box 2012. The engineering toolbox: Tools and basic information for design, engineering and construction of technical applications: Accessed on March 22, 2012, at http://www.EngineeringToolBox.com.

Gehlin, S. 2002. *Doctoral Thesis: Thermal Response Test – Method, Development and Evaluation*. Luleå: Luleå University of Technology.

GSHPA 2011. *Guideline for closed loop vertical borehole heat exchanger design, installation and material standards*. Milton Keynes: Ground source heat pump system association – National Energy Center.

Hakagerodur-geothermal 2012. Hakagerodour-geothermal: Handling book for borehole heat exchangers Technical details of geothermal pipes; Model: Geotherm PE-100. Accessed on March, 12, 2012 by email from Hakagerodour-geothermal AG.

Hellström, G. 1991. *Ph.D. Thesis: Ground heat storage thermal analyses of duct storage systems, I. Theory*. Lund: University of Lund.

Herrmann, V. J. 2008. *Doctoral Thesis: Ingenieurgeologische Untersuchungen zur Hinterfüllung von Geothermie-Bohrungen mit Erdwärmesonden. Karlsruhe: Karlsruhe Institute of Technology (KIT).*

Ingersoll, L. R., Zobel, O. J., Ingersoll, A. C. 1954. *Heat Conduction with Engineering*. Geological and Other Applications. New York: McGraw-Hill.

Jun, L., Xu, Z., Jun, G. and Jie Y. 2009. Evaluation of heat exchange rate of GHE in geothermal heat pump systems. *Renewable Energy* 34 (12): 2898–2904.

Lamarche, L., Kajl, S., Beauchamp, B. 2010. A review of methods to evaluate borehole thermal resistances in geothermal heat-pump systems. *Geothermics* 39: 187200.

Lee C., Lee K., Choi H., Choi H. P. 2010. Characteristics of thermally-enhanced bentonite grouts for geothermal heat exchanger in South Korea. *Science China: Technological Sciences* 53(1): 123–8.

Lee, C., Park, M., Nguyen, T., Sohn, B., Choi, J. M., Choi, H. 2011. Performance evaluation of closed-loop vertical

ground heat exchangers by conducting in-situ thermal response tests. *Renewable Energy* 42: 77–83.

Molina-Giraldo, N., Bayer, P., Blum, P. Zhu, K., Fang, Z. 2010. A moving finite line source model to simulate borehole heat exchangers with groundwater advection. *International Journal of Thermal Sciences* 50: 2506–2513.

Paul, N.D. 1996. *M.Sc. Thesis: The Effect of Grout Thermal Conductivity on Vertical Geothermal Heat Exchanger Design and Performance*. Vermillion, SD: South Dakota University

Reuß, M., Proell, M., Koenigsdorff, R. 2011. *Quality control of borehole heat exchanger systems*. Espoo: IEA ECES Annex 21 meeting.

Roussel, N. & Le Roy, R. 2005. The Marsh cone: a test or a rheological apparatus?. *Cement and Concrete Research* 35(5): 823–830.

Sharqawy, M.H., Mokheimer, E.M., Badr, H.M., 2009. Effective pipe-to-borehole thermal resistance for vertical ground heat exchangers. *Geothermics* 38: 271–277.

Sibelco 2012. Sibelco Benelux: Handling book for silica sand, physical characteristics of sand M-32 one grain size. Accessed on March, 7, 2012.

TIMCAL 2012. Personal communication 03.07.2012. Graphite & Carbon Manufacturer TIMCAL Ltd., Switzerland.

VDI-Richtlinie 2001a. *Thermal use of the underground, Blatt 2*. Düsseldorf: Verain Deutscher Ingenieure, VDI-Verlag.

VDI-Richtlinie 2001b. *Thermal use of the underground, Blatt 3*. Düsseldorf: Verain Deutscher Ingenieure, VDI-Verlag.